

## Investigating biodegradation of polyethylene and polypropylene microplastics in Tehran DWTPs

Fatemeh Tabatabaei<sup>a</sup>, Roya Mafigholami<sup>a,\*</sup>, Hamid Moghimi<sup>b</sup> and Sanaz Khoramipoor<sup>a</sup>

<sup>a</sup> Faculty of Environmental Science and Engineering, Islamic Azad University, West Tehran Branch, Tehran, Iran

<sup>b</sup> Department of Microbiology, University of Tehran, Tehran, Iran

\*Corresponding author. E-mail: r.mafigholami@wtiau.ac.ir

### ABSTRACT

Microplastic (MP) pollution is a growing concern and various methods are being sought to alleviate the level of pollution worldwide. This study investigates the biodegradation capacity of MPs by indigenous microorganisms of raw water from Tehran drinking water treatment plants. By exposing polypropylene (PP) and polyethylene (PE) MPs to selected microbial colonies, structural, morphological, and chemical changes were detected by scanning electron microscope (SEM), cell weight measurement, Fourier transform infrared (FTIR), Raman spectroscopy test, and thermal gravimetric analysis (TGA). Selected bacterial strains include *Pseudomonas protegens* strain (A), *Bacillus cereus* strain (B), and *Pseudomonas protegens* strain (C). SEM analysis showed roughness and cracks on PP MPs exposed to strains A and C. However, PE MPs exposed to strain B faced limited degradation. In samples related to strain A, the Raman spectrum was completely changed, and a new chemical structure was created. Both TGA and FTIR analysis confirmed changes detected by Raman analysis of PP and PE MPs in chemical changes in this study. The results of cell dry weight loss for microbial strains A, B, and C were 13.5, 38.6, and 25.6%, respectively. Moreover, MPs weight loss was recorded at 32.6% for PP MPs with strain A, 13.3% for PE MPs with strain B, and 25.6% for PP MPs with strain C.

**Key words:** biodegradation, FTIR, microplastic, Raman spectroscopy, SEM, TGA

### HIGHLIGHTS

- Microbial strains found in water treatment plants for MP biodegradation are used.
- PE and PP MPs in the biodegradation process are compared.

## 1. INTRODUCTION

Plastics are synthetic polymers that usually contain chemicals to have better performance. They are produced from petrochemical refineries and vary in density and plasticity (Costa *et al.* 2016). However, in certain environmental conditions, they are susceptible to undergo weathering and lose some of their chemical bonds (Browne *et al.* 2007). The crushing and decomposition of these plastics turn them into tiny microscopic particles called microplastics (MPs; Lwanga *et al.* 2017), ranging from 1 to 5,000  $\mu\text{m}$  in their longest end (Koelmans *et al.* 2019). Considering the increasing production of plastic products and the adverse effects of MPs on humans (gastrointestinal problems, endocrinal disruption, and respiratory problems) and other organisms (gut blockage, oxidative stress, reduced fecundity, and behavioral alteration), addressing such pollutants has become more crucial than ever (Nanthini devi *et al.* 2022; Emenike *et al.* 2023). These particles can also reduce the nitrogen cycle in soil, increase soil pH, and enter the food chain (Li *et al.* 2023a). Generally, MPs have been investigated in multiple freshwater and saline water resources including rivers (Cook *et al.* 2021; Stride *et al.* 2023a), wetlands (Mahdian *et al.* 2023), urban water infrastructures (Stride *et al.* 2023b), or nearshore regions (Abolfathi *et al.* 2020).

As drinking water treatment plants (DWTPs) are considered a reliable source of water supply for people, it is imperative to examine whether treated water is contaminated with MPs. Recent studies have detected MPs in DWTPs and tap water, raising concerns about the effectiveness of DWTPs in removing MPs at a desirable degree (Pivokonsky *et al.* 2018; Novotna *et al.* 2019; Jinkai *et al.* 2021). Therefore, it is necessary to investigate MPs reduction in DWTPs. Growing evidence indicates that microorganisms play a crucial role in decomposing plastics across various environments, including soil, sediments, seawater, and compost (Chen *et al.* 2023; Li *et al.* 2023b; Peng *et al.* 2023). In fact, through biodegradation, microorganisms are used to

This is an Open Access article distributed under the terms of the Creative Commons Attribution Licence (CC BY 4.0), which permits copying, adaptation and redistribution, provided the original work is properly cited (<http://creativecommons.org/licenses/by/4.0/>).

decompose plastic. Currently, different microorganisms are being explored in order to enhance the rate of plastic degradation (Li *et al.* 2023c).

Microorganisms can grow in diverse conditions and use carbon as their energy source. It has been observed that some strains can produce enzymes to degrade synthetic polymers, and the nature and catalytic activity of these enzymes vary depending on the microbial species and strains (Auta *et al.* 2018a, 2018b). For instance, Auta *et al.* (2018a, 2018b) observed that *Bacillus* sp. and *Rhodococcus* sp., isolated from sediments near mangrove plant roots, could grow in the presence of MPs and reduce their mass. After 40 days of contact, *Bacillus* sp. and *Rhodococcus* sp. achieved a 6.4 and 4% reduction in MPs mass, respectively. This analysis was further confirmed using a Fourier transform infrared (FTIR) spectroscopy and scanning electron microscope (SEM), which revealed morphological and structural changes on the surface of MPs. Finally, the researchers concluded that these types of bacteria can utilize polypropylene (PP) as a carbon source.

In another study, Habib *et al.* (2022) investigated the growth potential and degradation of PP MPs by a strain of bacteria found in the Antarctic, specifically *Pseudomonas* sp. ADL 15 and *Rhodococcus* sp. ADL 36. Over a 40-day period in the Bushnell Haas medium, the weight loss and degradation rate of MPs were analyzed, and the biodegradation of MPs was assessed by analyzing structural changes via FTIR spectroscopy. After 40 days, the weight loss rate of MPs was reported 17.3% for ADL 15 and 7.3% for ADL 36. FTIR analysis revealed significant changes in the functional groups of PPs.

This study aimed to identify microbial strains in the raw water environment from Tehran DWTPs and investigate the interaction between microorganisms and MPs. This paper also aims to investigate the ability of microbial communities to biodegrade MPs. For the first time, native microorganisms present in raw water were used in this study to assess the potential of DWTPs to remove MPs.

## 2. MATERIALS AND METHODS

### 2.1. Materials

In this study, PP and PE ( $0.92 \text{ g cm}^{-3}$ ) granules were purchased from Marun Petrochemical Company (Tehran, Iran). Then, the granules were immersed in 0.1 mol HCl for 12 h to decompose the potential residues. After drying in an oven at  $60^\circ\text{C}$  for 2 h, granules were immersed in liquid nitrogen until they reached  $-196^\circ\text{C}$ . Afterward, they were rapidly milled with an ultra-centrifugal mill (ZM 200, Retsch®, Germany) to achieve micron-sized MPs (Munno *et al.* 2018; Pivokonsky *et al.* 2018). Finally, MPs were sieved into three different size categories including  $d > 75 \mu\text{m}$ ,  $75 > d > 150 \mu\text{m}$  and  $d < 150 \mu\text{m}$ . After sieving, prepared MPs were sent to be exposed to selected microbial colonies. The culture media used for microbial growth were made with  $1 \text{ g L}^{-1}$  ammonium chloride ( $\text{NH}_4\text{Cl}$ ),  $3 \text{ g L}^{-1}$  monopotassium phosphate ( $\text{KH}_2\text{PO}_4$ ),  $7 \text{ g L}^{-1}$  disodium phosphate ( $\text{Na}_2\text{HPO}_4$ ),  $0.5 \text{ g L}^{-1}$  sodium chloride ( $\text{NaCl}$ ),  $0.25 \text{ g L}^{-1}$  magnesium sulfate ( $\text{MgSO}_4 \cdot 7\text{H}_2\text{O}$ ),  $1 \text{ g L}^{-1}$  PP or PE,  $40 \mu\text{g L}^{-1}$  copper sulfate ( $\text{CuSO}_4 \cdot 5\text{H}_2\text{O}$ ),  $0.2 \mu\text{g L}^{-1}$  ferric chloride ( $\text{FeCl}_3 \cdot 6\text{H}_2\text{O}$ ),  $0.4 \mu\text{g L}^{-1}$  magnesium sulfate ( $\text{MnSO}_4 \cdot 5\text{H}_2\text{O}$ ),  $0.4 \mu\text{g L}^{-1}$  zinc chloride ( $\text{ZnCl}_2$ ),  $0.2 \mu\text{g L}^{-1}$  ammonium molybdate ( $(\text{NH}_4)_6\text{Mo}_7\text{O}_{24} \cdot 7\text{H}_2\text{O}$ ), and  $0.5 \mu\text{g L}^{-1}$  boric acid ( $\text{H}_3\text{BO}_3$ ) (Shirazi *et al.* 2023).

### 2.2. Sampling

The sampling method in this study is based on Bonetta *et al.* (2022) with minor changes according to the purpose of this study. From June to July 2022, three 100 mL samples were taken from the raw water of three different DWTPs in Tehran and fed from different water resources. Sampling bottles were made of glass in a dark color. In total, 9 samples comprising 2.7 L of samples were collected for bacterial identification. Samples were kept refrigerated within 24 h before being sent to microbial-related analysis.

### 2.3. MP biodegradation

Regarding the biodegradation of the identified polymers, the biodegradation process was carried out in a synthetic environment. Initially, after preparing the culture medium and sterilizing MPs using an autoclave, they were inoculated in a 500 mL Erlenmeyer flask along with 1 mL of water sample from the raw water of DWTPs and 100 mL of prepared culture medium. The flasks were placed on a shaker at a speed of 140 rpm and incubated for 1 month at  $37^\circ\text{C}$  in  $\text{pH } 7 \pm 0.5$  (Gong *et al.* 2018). After this period, colonies consisting of bacteria and fungi were observed in the culture medium. These colonies were purified and isolated, and the process of MPs inoculation and bacterial colony growth without the water sample was repeated for the second and third times. The samples were placed on the shaker for 9–12 weeks. The consortium of bacteria exhibiting the highest consumption of MPs was selected through primary screening based on the greatest weight loss of MPs. Among 20

bacteria tested, the three samples showing the highest efficiency were chosen for deoxyribonucleic acid (DNA) extraction and polymerase chain reaction (PCR) testing. Next, three samples containing the selected pure bacteria and MPs were inoculated into the culture medium and placed on a shaker for 3 months. In addition, two control samples were prepared alongside the main samples, with all conditions being similar except for the presence of bacteria. After the specified time, the weight of MPs was compared to that of before the exposure to determine the mass reduction and calculate the degradation rate. To assess the molecular bonds and analyze the structure of MPs, samples were filtered through a 0.45 µm membrane filter. In this regard, to eliminate possible bacteria on the filter samples, 96% ethanol diluted with 20 mL of distilled water was utilized. Next, the filters were placed in a glass petri dish for 30 min in an oven at 60°C. For further analysis, samples containing MPs were exposed to bacteria, as well as two control samples of PP and PE MPs without bacteria were prepared. Raman spectroscopy, FTIR analysis, and thermal gravimetric analysis (TGA) were performed to identify changes in molecular bonds. Additionally, a SEM was utilized to identify the morphology of the decomposed MPs (Rizzarelli *et al.* 2016; Mintenig *et al.* 2019).

#### 2.4. Microbial identification

For molecular identification and genomic DNA extraction, the desired isolates were first inoculated into a nutrient broth liquid culture medium and heated until reaching a suitable biomass. Subsequently, the cells were physically disrupted by beating the frozen biomass with liquid nitrogen, and the DNA was isolated through phenol–chloroform extraction (Oßmann *et al.* 2018). To achieve molecular identification of the isolates, the extracted DNA was amplified using PCR with the general primers 27F and 1492R. Horizontal electrophoresis was performed using a 1% agarose gel to assess sample purity. Finally, the target gene and its sequence were compared to sequences in the National Center for Biotechnology Information (NCBI) databases for identification (Oßmann *et al.* 2018).

#### 2.5. Investigating cell dry weight method

The growth kinetic of selected strains in dried weight in the culture medium comprising 1,000 mg of MPs signifies the consumption of MPs by the inoculated strains. Since the only carbon source in the medium is MPs, the amount of created biomass can indirectly mean the biodegradation of these particles. Hence, selected strains were inoculated in the culture medium containing 1,000 mg of MPs and incubated at 28°C for 30 days on a shaker at the speed of 150 rpm. After this step, the flask contents were centrifuged at 8,000 rpm and supernatants were disposed of. To measure the weight loss, the flask contents were poured on pre-weighed glass plates. Next, the plates were kept in 65°C for 48 h and weighed again. The weight loss was calculated using Equation (1), where  $W_0$  represents the initial weight in grams and  $W$  represents the weight of the remaining MPs (Shirazi *et al.* 2023).

#### 2.6. MPs weight loss

In this process, MPs weight loss can imply the biodegradation of these particles. To start, MPs were filtered through a 6 µm membrane filter (Hyundai Micro Co. Ltd, Korea). After washing MPs on filters, they were sterilized and dried as explained before. To reduce potential errors in this process, the temperature of the oven was maintained at 50°C to prevent loss of fatty acids, and all the membrane filters were weighed at the precision of 0.0001 g (CY314C, USA) and some membrane filters were dried in the oven as control samples to measure the effect of moisture loss on their weight. MPs weight loss was achieved by Equation (1):

$$\text{MPs weight loss} = \left( \frac{W_0 - W}{W_0} \right) \times 100 \quad (1)$$

#### 2.7. Investigating the biodegradation of MPs based on the CO<sub>2</sub> level

The carbon dioxide produced by microorganisms was captured using a sodium hydroxide (NaOH) solution, allowing for the determination of respiration level through titration or conductometry (Cerqueira *et al.* 2013). After transferring from the pre-culture medium to the primary culture medium, the inoculated bacteria were heated at 28°C and 150 rpm shaker for 21 days. For the second time, oxygen was injected into the glass. The amount of carbon dioxide produced was calculated based on the amount of acid consumed in the titration activity with three repetition steps at the end of 21 days. The amount of carbon

dioxide produced in mg was calculated based on Equation (2) (Cerqueira *et al.* 2013).

$$(V_B - V_A) \times (M_{\text{CO}_2}) \times M_{\text{HCl}} \times C_F \quad (2)$$

where  $V_B$  represents the volume of HCl consumed in the control,  $V_A$  represents the volume of HCl consumed in the sample, and  $C_F$  is a ratio equal to  $M_{\text{HCl}}/M_{\text{KOH}}$ .

### 2.8. Investigating the growth capacity of selected strains based on protein production

Measuring produced protein from the MPs biodegradation can indirectly represent the ability of selected bacteria in plastic degradation. For this process, the method developed by Lowry *et al.* (1951) was employed. In brief, four reagents were prepared including reagent A (2%  $\text{Na}_2\text{CO}_3$  in 0.1 mol NaOH), reagent B (0.5%  $\text{CuSO}_4 \cdot 5\text{H}_2\text{O}$  in 1% sodium tartrate), reagent C (mixture of 50 mL of reagent A with 1 mL of reagent B), and reagent D (same as reagent C, except for the omission of NaOH). A 100  $\mu\text{L}$  of the prepared culture medium was mixed with 1 mL of reagent C in a 1.5 mL vial and kept at room temperature for 15 min. Then, 0.1 mL of reagent D was added to the mixture and mixed for 45 s with a vortex. To create a protein assay standard curve, different concentrations of bovine serum albumin from 0.1 to 1  $\text{mg mL}^{-1}$  in deionized water were prepared, and the optical absorption of the medium was measured at a wavelength of 650 nm. Mentioned experiments were conducted in triplicate.

## 3. RESULTS AND DISCUSSION

### 3.1. Identification of selected biomass strains

After evaluating the effectiveness of 20 different strains of bacteria, 3 samples with the highest efficiency were selected for DNA extraction and PCR testing. The microbial community analysis, focusing on the biodegradation of PP and PE MPs, was carried out using the NCBI database. The analysis revealed the presence of the strains *Pseudomonas protegens* (A), *Bacillus amyloliquefaciens* (B) and *Bacillus cereus* (C) with a 99, 99 and 100% similarity, respectively. Strain A has been observed as a biofilm on MPs surface found in Ganjiang River, China (Hu *et al.* 2021). In another study, bacterial strain B was observed to be effective on polystyrene (PS) MPs biodegradation (Kang *et al.* 2023). Moreover, strain C has been effective in the biodegradation of low-density polyethylene in other studies. However, they have found the bacteria in the soil environment (Jayan *et al.* 2023).

### 3.2. Thermogravimetric analysis

In most of the studies of MPs investigation in DWTPs, PP and PE MPs have been detected as the most abundant polymer types in raw water samples comprising more than 60% of detected MPs (Adib *et al.* 2021; Jung *et al.* 2022; Islam *et al.* 2023). So, in this study, PP and MPs were selected for biodegradability investigations. Thermal properties of PE and PP MPs were examined using the TGA test before and after exposure to bacteria. The results of this test for PP and PE-based samples are presented in Figures 1 and 2, respectively.

In Figure 1, the weight loss observed corresponds to the thermal decomposition of the PP chemical chain. In the control sample, according to the derivative thermogravimetric (DTG) curve, this decomposition occurred at approximately 457°C. This weight loss at this temperature aligns with findings reported in similar articles (Jung *et al.* 2010; Żwieręło *et al.* 2020). It is evident from the figure that the thermogram of sample C closely resembles that of the control sample. This indicates that the bacteria in this sample probably has a minimal impact on the structure of the polymer. The microbial strain caused the breakdown of some long chains, resulting in a slight reduction in thermal stability. The weight loss of this polymer at 800°C increased slightly from 7.97 to 8.13 mg. In the TGA test results of sample A, it is clear that the bacterial strain in this sample attacked the PP polymer structure, leading to significant changes. One notable change observed in the thermograms is an additional weight loss in the TGA curve, accompanied by an endothermic peak in the DTG curve between 50 and 150°C (DTG peak at 97°C). This weight loss and endothermic peak can be attributed to eliminating water absorbed on the surface. PP is inherently hydrophobic due to its long hydrocarbon chains. Therefore, no water absorption effect was observed in the TGA curve of the control sample at temperatures lower than 200°C. However, when the PP MPs were exposed to the bacteria in sample A, structural changes occurred, resulting in the creation of polar groups on the polymer's surface. As a result, the polymer became hydrophilic and exhibited water absorption. As depicted in the thermograms, sample A experienced weight loss in the temperature 440–520°C (DTG peak at 460°C), corresponding to the thermal decomposition of intact PP structure.

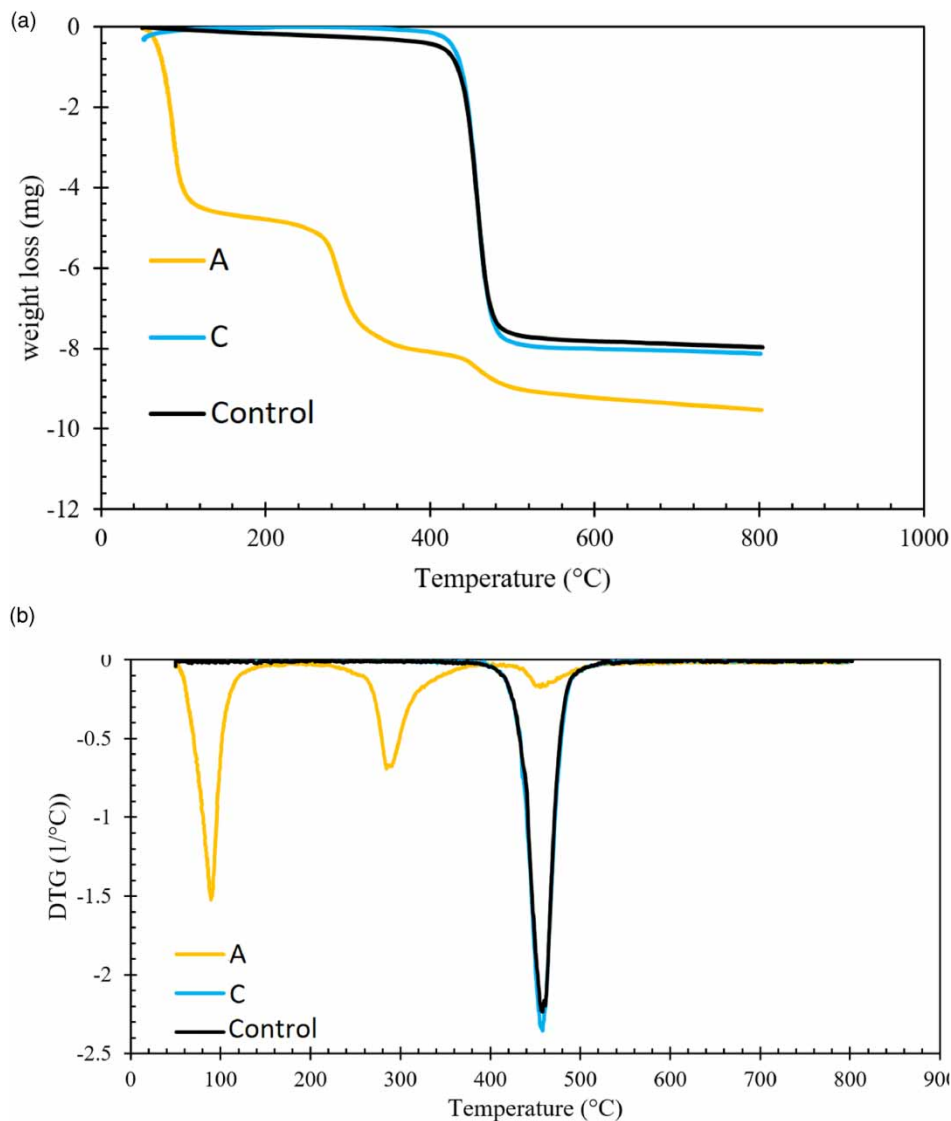


**Figure 1** | (a) TGA and (b) DTG curves of PP sample, before and after exposure to A and C.

Another weight loss stage was observed in the temperature of 220–375°C (DTG peak at 281°C), indicating the thermal decomposition of PP chemical chains broken by bacteria in this sample.

Moving on to the TGA and DTG curves for the PE shown in Figure 2, it is evident that the thermal decomposition of this polymer resulted in a single stage of weight loss in the temperature of 400–530°C (DTG peak at 476°C). In the TGA curve of strain B, although the weight loss occurred at almost the same temperature as the control sample, the weight loss in strain B was greater than that of the control sample. Specifically, the weight loss increased from approximately 3.9 mg in the control sample to about 5.9 mg in sample B. These results confirm that the selected strains used in sample B did not destroy the main structure of the PE but rather produced products with lower thermal stability than the control sample.

### 3.3. Raman analysis

Changes in chemical bonds in these samples were investigated using Raman spectroscopy. Obtained spectra of PE and PP MPs, before and after the exposure, are shown in Figures 3 and 4, respectively.

In the obtained spectra, the stretching vibrations of C–C bonds are at 1,059, 1,079 and 1,126  $\text{cm}^{-1}$ . Additionally, the rocking vibration of  $\text{CH}_2$  groups and the twisting vibration of C–H bonds have made peaks at 1,166 and 1,293  $\text{cm}^{-1}$ . The peak at



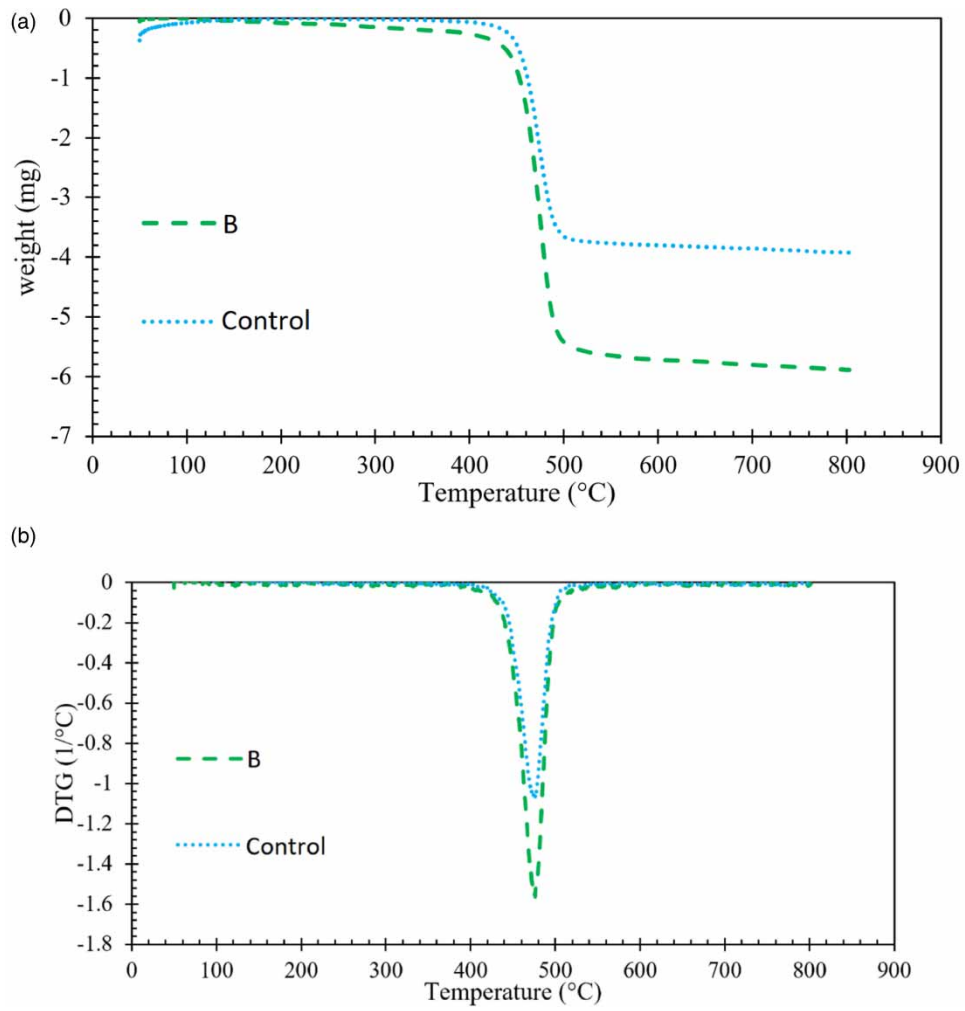


**Figure 2** | (a) TGA and (b) DTG curves of PE sample, before and after exposure to C.

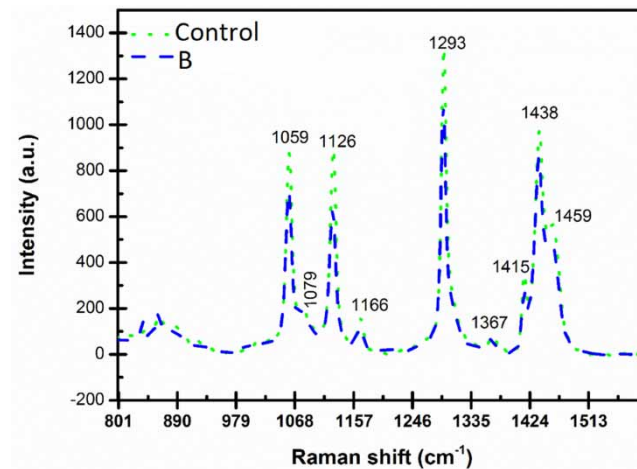


**Figure 3** | The Raman spectra of control PE MPs, before and after exposure to bacteria (B).

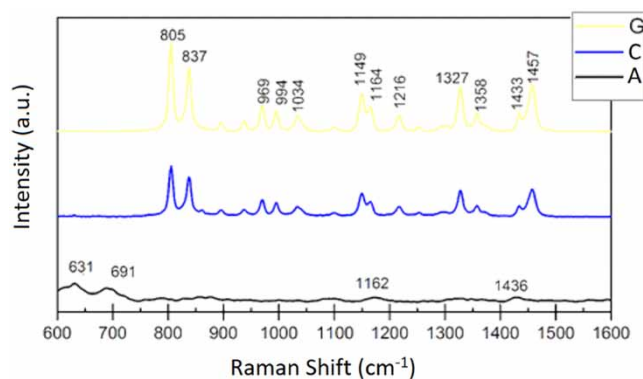


**Figure 4** | Raman spectra obtained from PE control sample (G) and the samples exposed to bacteria (A and C).

$1,367\text{ cm}^{-1}$  corresponds to the wagging vibration of  $\text{CH}_3$  bonds (Visentin *et al.* 2006). In addition, the bending vibrations of  $\text{CH}_2$  bonds have created peaks at  $1,415$ ,  $1,438$  and  $1,459\text{ cm}^{-1}$ . These spectra are consistent with the previous study on PE (Furukawa *et al.* 2006), confirming the existence of the PE structure.

Figure 3 illustrates that in sample B, exposed to bacteria, there is a reduction in peak intensity without any shift in peak positions, suggesting the potential breakage of PE chains. However, the bacteria have not been able to change the structure of PE and form new structures. Figure 4 presents the Raman spectra of PE samples.

In the Raman spectrum of the PP control sample, the stretching vibrations of C–C bonds appeared at  $805$  and  $1,034\text{ cm}^{-1}$ . Also, the rocking vibration of  $\text{CH}_3$  groups resulted in peaks at  $837$  and  $969\text{ cm}^{-1}$  (Jung *et al.* 2018). In addition, the bending vibrations of  $\text{CH}_2$  bonds were evident in peaks at  $994$ ,  $1,149$ , and  $1,164\text{ cm}^{-1}$  (Cerqueira *et al.* 2013). The peak at  $1,216\text{ cm}^{-1}$  can also be attributed to the combined effects of the wagging vibration of C–H bonds, the twisting vibration of  $\text{CH}_2$  groups, and the stretching vibration of C–C bonds. The twisting vibration of  $\text{CH}_2$  groups and the wagging vibration of  $\text{CH}_3$  groups created peaks at  $1,327$  and  $1,358\text{ cm}^{-1}$ , respectively. The bending vibration of  $\text{CH}_2$  groups intensified the peaks at  $1,433$  and  $1,457\text{ cm}^{-1}$  (Jung *et al.* 2018). Figure 4 indicates that the same peaks were also present in sample C, suggesting that the overall polymer structure remained unchanged in the presence of bacteria. However, in sample A, the spectrum was completely changed, and a new chemical structure was obtained due to the combination of polymer and bacteria. In the spectrum of sample A, the bending vibration of C–H bonds in Raman showed shifts at  $631$  and  $691\text{ cm}^{-1}$ . Furthermore, due to the structural changes induced by the bacteria, original peaks at  $1,149$  and  $1,433\text{ cm}^{-1}$  in PP were shifted to  $1,162$  and  $1,436\text{ cm}^{-1}$ , respectively (Jung *et al.* 2018).

#### 3.4. FTIR analysis

To accurately determine the changed structure from the reaction between PP and bacteria in sample A, more analyses are needed. FTIR was utilized to investigate the links within the structure of these samples, and the results are shown in Figures 5 and 6.

In Figure 5, the spectrum of the obtained samples implies a broad peak in the range of  $3,000$ – $3,700\text{ cm}^{-1}$  wave number, which can be attributed to the stretching vibration of hydroxyl bonds (O–H). This peak exists due to the surface absorption of water on these polymers (Muthuselvi *et al.* 2018). Also, multiple absorption peaks observed in wave numbers ranging from  $2,700$  to  $3,000\text{ cm}^{-1}$  correspond to the stretching vibration of C–H bonds in  $\text{CH}$ ,  $\text{CH}_2$ , and  $\text{CH}_3$  groups, as reported in similar studies (Shahmoradi *et al.* 2020). Furthermore, according to the findings of a similar study (Jung *et al.* 2018), the peak at approximately  $1,600\text{ cm}^{-1}$  is related to the bending vibration of O–H bonds (surface adsorbed water), while the peak at around  $1,380\text{ cm}^{-1}$  is attributed to the bending vibration of C–H bonds. Also, the wagging vibration of C–H bonds is indicated by the presence of an absorption peak at wave number  $1,120\text{ cm}^{-1}$ , while the stretching vibration of C–C bonds illustrates an absorption peak at wave number  $1,000\text{ cm}^{-1}$  (Shahmoradi *et al.* 2020). The broad peak at a wave number below  $800\text{ cm}^{-1}$  may be attributed to the stretching vibration of C–CH bonds. By comparing these spectra, it is evident that the FTIR spectrum of sample C closely resembles that of the reference sample, albeit with reduced peak intensities for certain vibrations such as C–H and C–C. This suggests that in the presence of bacteria in sample C, changes in PP chemical chains have been created, resulting in a decrease in peak intensity. The absence of new peaks confirms the absence of new bonds in the structure of PP.

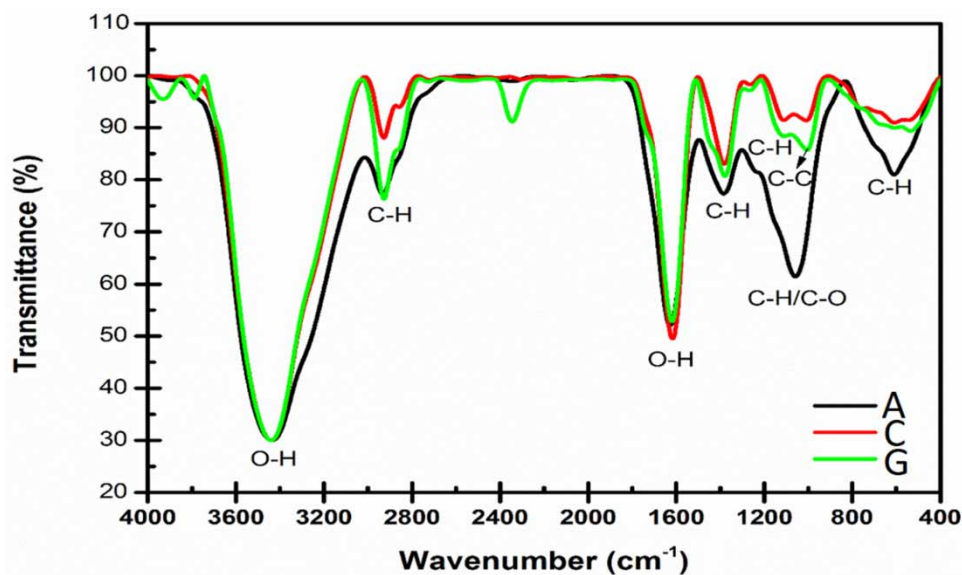


**Figure 5** | FTIR spectrum applied on PP as control sample (G) and the samples exposed to bacteria (A and C).

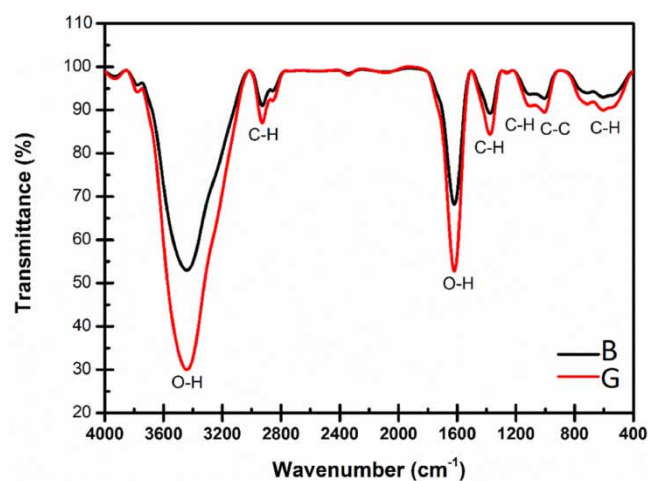


**Figure 6** | The spectra obtained from FTIR analysis of control PE samples vs. PP MPs exposed to bacteria (B).

However, in sample A, notable changes in peak intensities can be observed, along with the creation of a peak at approximately  $1,050\text{ cm}^{-1}$ . This peak can be attributed to the stretching vibration of C–O bonds in this sample. This peak can confirm the results of Raman analysis and TGA, which indicated a complete change in PP structure and the formation of new functional groups in the presence of bacteria. Figure 6 shows the FTIR spectrum of PE. According to Figure 6, the spectrum of the studied samples reveals several characteristics: (1) a broad peak in the wave number of  $3,000\text{--}3,700\text{ cm}^{-1}$  is observed, which corresponds to the stretching vibration of the hydroxyl bonds (O–H). This peak is attributed to the surface absorption of water on the polymers. Additionally, there are absorption peaks between wavenumber  $2,800$  and  $3,000\text{ cm}^{-1}$ , which are related to the symmetric and asymmetric stretching vibration of C–H bonds in CH groups.

The peak at approximately  $1,600\text{ cm}^{-1}$  is related to the bending vibration of O–H bonds (surface absorbed water), while the peak at  $1,350\text{ cm}^{-1}$  corresponds to the bending vibration of C–H bonds. In this sample, the wagging vibration of C–H bonds is represented by a peak at around  $1,115\text{ cm}^{-1}$ , and the stretching vibration of C–C bonds appears as an absorption peak at approximately  $1,010\text{ cm}^{-1}$ . Furthermore, the broad peaks observed at wave number below  $800\text{ cm}^{-1}$  can be attributed to



the stretching vibration of C–CH bonds. By comparing these spectra, it is evident that the FTIR spectrum of sample B closely resembles that of the control sample, with a reduction in intensity observed for certain peaks, such as those associated with C–H and C–C vibrations. Therefore, it can be concluded that due to the breaking of PE chemical chains in the presence of bacteria in sample B, only the intensity of the peaks has been affected, and the absence of a new peak confirms the absence of new bonds in the structure of this material. This result is in line with the results of Raman analysis and TGA.

### 3.5. SEM test results

The changes in the surface morphology of PP and PE MPs were investigated, as well as the growth of biofilm on them using an SEM with a voltage of 20 kW. In images obtained SEM from the samples exposed to microbial treatment for 3 months, notable differences can be observed compared to the control sample of PP (Figure 7). The surface of PP exhibits an uneven texture with numerous ridges. At higher magnification, it is evident that there are discontinuous holes and smooth areas between these ridges. In Figure 7 – G1, bacteria surround the surface of PP mounds. Bacteria appear both in single and congested forms. The comparison of fractures and holes of similar sizes between the control sample and PP MPs with bacteria A (Figure 7 – G1) shows that the presence of these features is much more pronounced. In PP MPs with bacteria C (Figure 7 – G2), most bacteria are found in flat areas and between surface protrusions (Klun *et al.* 2023). The most prominent changes are evident in the form of uneven pits and various irregularities in the sample with PP MPs and bacteria A, as well as the formation of horizontal cracks in the sample with bacteria C (de Villalobos *et al.* 2022). In both samples, the microbial strains adhere to the surface of the MPs and surround the surface, resulting in damage and erosion of the particles. Figure 8 illustrates the surface morphology of the PE control sample. The MP surface exhibits unevenness with numerous ridges. However, in the sample exposed to bacteria (C), the surface is smooth, and a significant part of the unevenness has been flattened. However, compared to the other two bacterial strains, the degree of changes indicates the lower ability of this strain to break down the PE chemical structure. Appearance changes of MPs in this study are in line with Nwuzor *et al.* (2023), which observed cracks and disruptions in MPs surface after incubation with bacteria.

### 3.6. Bacteria performance

The results of the cell weight measurement test showed that the average weight loss of the PP sample exposed to bacterial strains A and C were 38.6 and 25.6%, respectively. The greater weight loss observed in the presence of microbial strain A compared to strain C indicates that strain A has a more significant effect on the degradation of the chemical structure of PP MPs. Furthermore, the average cell weight loss for PE MPs exposed to strain B was 13.5%, which was the lowest decrease

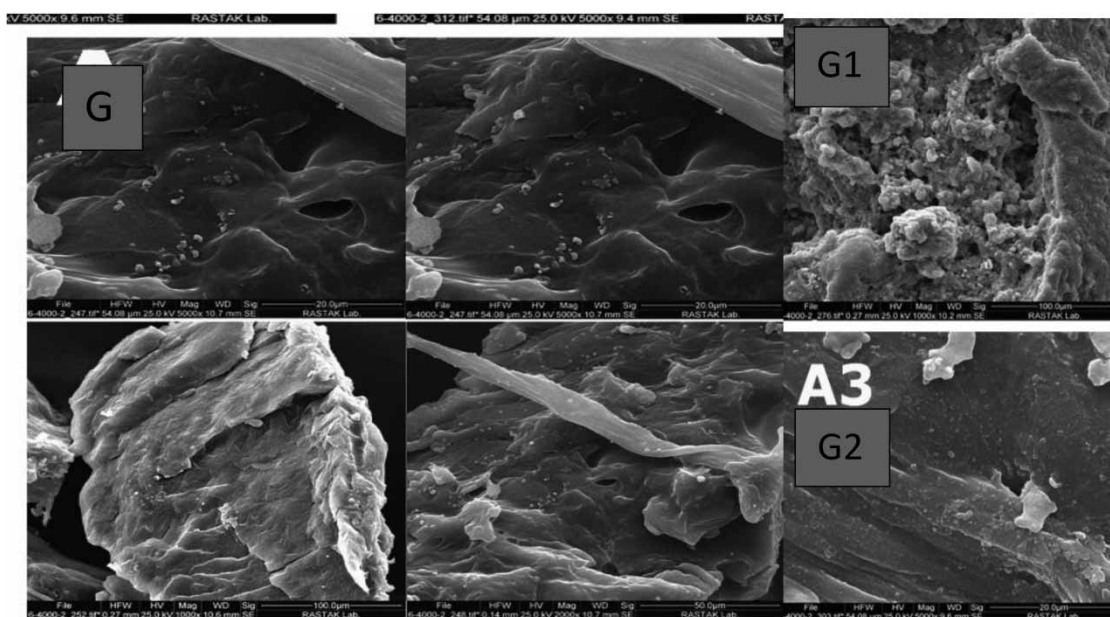


**Figure 7** | Control sample PP (G) (G1 represents PP MPs with bacteria A and G2 represents PP MPs with bacteria C).

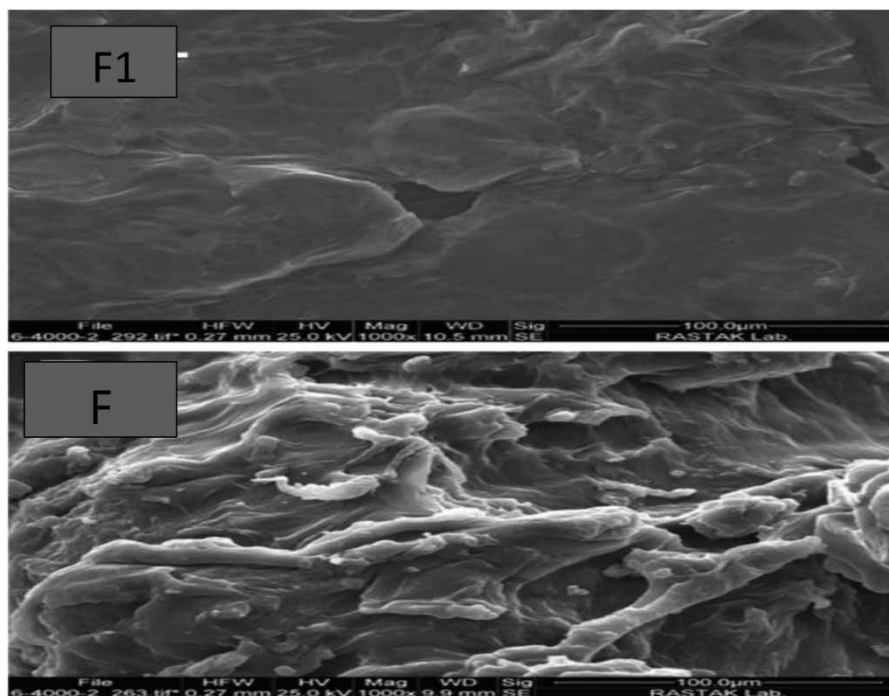


**Figure 8** | F represents PE control sample and F1 represents PE MPs with bacteria C.

among the investigated strains. In a recent study, [Tiwari et al. \(2024\)](#) observed that *Achromobacter xylosoxidans* reduced PE MPs dry weight by 26.7%. This indicates that strain C is not effective enough to biodegrade PE MPs and other strains from other locations may be more effective. In addition, the test results for the amount of CO<sub>2</sub> produced for the samples exposed to strains A, C, and B were 3.03, 2.36, and 0.83 g L<sup>-1</sup>, respectively. Also, the results of the test measuring the growth of the strains based on protein production indicated average protein yields of 4.1, 3.01, and 1.48 g L<sup>-1</sup> for the samples exposed to strains A, C, and B, respectively. [Table 1](#) shows MPs weight loss exposed to strains A, B, and C.

Weight loss of MPs was investigated based on 1,000 mg of the initial addition of particles to the samples. Based on [Table 1](#), strain A had the most effect on biodegradation among the other two strains with a 32.6% decrease in the weight of PP MPs, while strain B had a lower impact on PE MPs weight loss with a 13.3% decrease. These findings indicate that strain A has a greater effect on the destruction of MPs chemical structures than the other two strains. In a similar study, [Auta et al. \(2018a, 2018b\)](#) exposed PP nanoplastics to *Bacillus* sp. and *Rhodococcus* sp. after 40 days of incubation, only 6%. Likewise, in another study by [Tiwari et al. \(2023\)](#), PE MPs were incubated with *BreviBacillus brevis* for 35 days, which resulted in a 19.8% reduction in MPs weight. So, the obtained result in this study is comparable to that of mentioned similar studies.

#### 4. FUTURE STUDIES

This study investigated the most abundant polymer types in MPs; however, other polymers that are predominantly found in DWTPs need to be investigated in terms of biodegradation capacity including PS, polyethylene terephthalate, and polyvinyl chloride. Moreover, bacterial strain detection should be investigated in DWTPs of other geographical locations to find out

**Table 1** | Weight loss of MPs exposed to strains A, B, and after 3 months

Strain	Polymer type	Weight loss
A	PP	0.674 ± 0.012
B	PE	0.867 ± 0.022
C	PP	0.744 ± 0.007

whether it exists another bacterial strain that has a more efficient effect on MPs biodegradation. In addition, this study collected raw water samples in a single period of time within a year, while sampling in multiple times of a year may alter the results in bacterial selection for biodegradation.

## 5. CONCLUSIONS

It can be concluded from the overall test results that exposure of MPs to strains A, B, and C for 3 months demonstrates that these strains adhere to the surface of both PE and PP MPs, leading to chemical damage and erosion. Various irregularities and unevenness of pits were observed in the samples containing PP MPs treated with strain A, and the chemical structure of PP MPs was changed according to FTIR and Raman analysis and underwent a complete degradation with the creation of new functional groups. On the other hand, in the samples containing PE MPs treated with strain B, noticeable changes were observed to some extent and a lower ability of this strain was observed to break down the PE structure compared to the other strains used in this study. In samples with strains B and C, the general structure of the polymer was not changed by the bacteria present. The results of cell dry weight loss also indicated that the weight loss of MPs in the presence of microbial strain A was more significant compared to microbial strain C. The average weight loss of cells observed for PE MPs exposed to strain B was 13.5%, the lowest among the strains examined in this research. In addition, after 3 months of incubation, MPs exposed to bacteria experienced weight loss. PP MPs weight decreased by 32.6% when exposed to strain A, while the decrease rate was lower when exposed to strain B (25.6%). On the other hand, strain B could not have a significant impact on PE MPs biodegradation and caused a 13.3% decrease in their weight.

## ACKNOWLEDGEMENTS

We want to thank all the professors and friends who, with complete honesty and sincerity, supported us scientifically and technically during the implementation of this research. All the expenses of this study were supported by Fatemeh Tabatabaei. We appreciate Islamic Azad University, West Tehran Branch for providing equipment to conduct this study.

## AUTHOR CONTRIBUTIONS

All authors equally contributed to preparing this article.

## DATA AVAILABILITY STATEMENT

All relevant data are included in the paper or its Supplementary Information.

## CONFLICT OF INTEREST

The authors declare there is no conflict.

## REFERENCES

- Abolfathi, S., Cook, S., Yeganeh-Bakhtiary, A., Borzooei, S. & Pearson, J. 2020 Microplastics transport and mixing mechanisms in the nearshore region. *Coastal Engineering Proceedings* **36**, 63.
- Adib, D., Mafiqholami, R. & Tabeshkia, H. 2021 Identification of microplastics in conventional drinking water treatment plants in Tehran, Iran. *Journal of Environmental Health Science and Engineering* **19**, 1817–1826.
- Auta, H. S., Emenike, C. & Fauziah, S. 2018a Distribution and importance of microplastics in the marine environment: A review of the sources, fate, effects, and potential solutions. *Environment International* **102**, 165–176.
- Auta, H. S., Emenike, C. U., Jayanthi, B. & Fauziah, S. H. 2018b Growth kinetics and biodeterioration of polypropylene microplastics by *Bacillus sp.* and *Rhodococcus sp.* isolated from mangrove sediment. *Marine Pollution Bulletin* **127**, 15–21.
- Bonetta, S., Pignata, C., Gasparro, E., Richiardi, L., Bonetta, S. & Garraro, E. 2022 Impact of wastewater treatment plants on microbiological contamination for evaluating the risks of wastewater reuse. *Environmental Sciences Europe* **34**, 20.
- Browne, M. A., Galloway, T. & Thompson, R. 2007 Microplastic – an emerging contaminant of potential concern? *Integrated Environmental Assessment and Management* **3** (4), 559–561.
- Cerqueira, M. A., Souza, B. W. S., Teixeira, J. A. & Vicente, A. A. 2013 Utilization of galactomannan from *Gleditsia triacanthos* in polysaccharide-based films: Effects of interactions between film constituents on film properties, food and bioprocess. *Technology* **6**, 1600–1608.
- Chen, B., Zhang, Z., Wang, T., Hu, H., Qin, G., Lu, T., Hong, W., Hu, J., Penueles, J. & Qian, H. 2023 Global distribution of marine microplastics and potential for biodegradation. *Journal of Hazardous Materials* **451**, 131198.

- Cook, S., Abolfathi, S. & Gilbert, N. I. 2021 Goals and approaches in the use of citizen science for exploring plastic pollution in freshwater ecosystems: A review. *Freshwater Science* **40** (4), 567–579.
- Costa, J. P., Santos, P. S. M., Duarte, A. C. & Rocha-Santos, T. 2016 (Nano) plastics in the environment – Sources, fates and effects. *Science of the Total Environment* **567**, 15–26.
- de Villalobos, N. F., Costa, M. C. & Marín-Beltrán, I. 2022 A community of marine bacteria with potential to biodegrade petroleum-based and biobased microplastics. *Marine Pollution Bulletin* **185** (A), 114251.
- Emenike, E. C., Okorie, C. J., Ojeyemi, T., Egbemhenge, A., Iwuozor, K. O., Saliu, O. D., Okoro, H. K. & Adeniyi, A. G. 2023 From oceans to dinner plates: The impact of microplastics on human health. *Heliyon* **9** (110), e20440.
- Furukawa, T., Sato, H., Kita, Y., Matsukawa, K., Yamaguchi, H. & Ochiai, S. 2006 Molecular structure, crystallinity and morphology of polyethylene/polypropylene blends studied by Raman mapping, scanning electron microscopy, wide angle X-ray diffraction, and differential scanning calorimetry. *Polymer Journal* **38**, 1127–1136.
- Gong, J., Kong, T., Li, Y., Li, Q., Li, Z. & Zhang, J. 2018 Biodegradation of microplastic derived from poly(ethylene terephthalate) with bacterial whole-cell biocatalysts. *Polymers* **10** (12), 1326.
- Habib, R. Z., Ramachandran, T., Hamed, F., Al Kindi, R., Ismail Mourad, A.-H. & Thieman, T. 2022 Microplastic in an arid region: Identification, quantification and characterization on and alongside roads in Al Ain, Abu Dhabi, United Arab Emirates. *Journal of Environmental Protection* **13**, 671–688.
- Hu, H., Jin, D., Yang, Y., Zhang, J., Ma, C. & Qiu, Z. 2021 Distinct profile of bacterial community and antibiotic resistance genes on microplastics in Ganjiang River at the watershed level. *Environmental Research* **200**, 111363.
- Islam, M. S., Islam, Z., Molla Jamal, A. H. M. S. I., Momtaz, N. & Beauty, S. A. 2023 Removal efficiencies of microplastics of the three largest drinking water treatment plants in Bangladesh. *Science of the Total Environment* **895**, 165155.
- Jayan, N., Skariyachan, S. & Sebastian, D. 2023 The escalated potential of the novel isolate *Bacillus cereus* NJD1 for effective biodegradation of LDPE films without pre-treatment. *Journal of Hazardous Materials* **455**, 131623.
- Jinkai, X., Samaei, S. H.-A., Chen, J., Doucet, A. & Tsun Wai Ng, K. 2021 What have we known so far about microplastics in drinking water treatment? A timely review. *Frontiers of Environmental Science & Engineering* **16** (5), 58.
- Jung, S.-H., Cho, M.-H., Kang, B.-S. & Kim, J.-S. 2010 Pyrolysis of a fraction of waste polypropylene and polyethylene for the recovery of BTX aromatics using a fluidized bed reactor. *Fuel Processing Technology* **3**, 277–284.
- Jung, M. R., Horgen, F. D., Orski, S. V., Rodriguez, V., Beers, K. L. & Balazs, G. H. 2018 Validation of ATR FT-IR to identify polymers of plastic marine debris, including those ingested by marine organisms. *Marine Pollution Bulletin* **127**, 704–716.
- Jung, J.-W., Kim, S., Kim, Y.-S., Jeong, S. & Lee, S. 2022 Tracing microplastics from raw water to drinking water treatment plants in Busan, South Korea. *Science of the Total Environment* **825**, 154015.
- Kang, M.-G., Kwak, M.-J. & Kim, Y. 2023 Polystyrene microplastics biodegradation by gut bacterial *Enterobacter hormaechei* from mealworms under anaerobic conditions: Anaerobic oxidation and depolymerization. *Journal of Hazardous Materials* **459**, 132045.
- Klun, B., Rozman, U. & Kalčíková, G. 2023 Environmental aging and biodegradation of tire wear microplastics in the aquatic environment. *Journal of Environmental Chemical Engineering* **11** (5), 110604.
- Koelmans, B., Pahl, S., Backhaus, T., Bessa, F., van Calster, G., Contzen, N., Cronin, R., Galloway, T., Hart, A., Henderson, L., Kalčíková, G., Kelly, F., Kolodziejczyk, B., Marku, E., Poortinga, W., Rillig, M., van Sebille, E., Steg, L., Steinhorst, J., Steidl, J., Syberg, K., Thompson, R., Wagner, M., van Wezel, A., Wyles, K. & Wright, S. 2019 *A Scientific Perspective on Microplastics in Nature and Society*. SAPEA, Science Advice for Policy by European Academies, Berlin, Germany, p. 173.
- Li, Z., Yang, Y., Chen, X., He, Y., Bolan, N., Rinklebe, J., Lam, S. S., Peng, W. & Sonne, C. 2023a A discussion of microplastics in soil and risks for ecosystems and food chains. *Chemosphere* **313**, 137637.
- Li, Y., Liu, Q., Junaid, M., Chen, G. & Wang, J. 2023b Distribution, sources, transportation and biodegradation of microplastics in the soil environment. *TrAC Trends in Analytical Chemistry* **164**, 117106.
- Li, S., Yang, Y., Yang, S., Zheng, H., Zheng, Y., Nagarajan D, M. J., Varjani, S. & Chang, J. S. 2023c Recent advances in biodegradation of emerging contaminants – microplastics (MPs): Feasibility, mechanism, and future prospects. *Chemosphere* **331**, 138776.
- Lowry, O. H., Rosebrough, N., Farr, A. L. & Randall, R. 1951 Protein measurement with the Folin phenol reagent. *Journal of Biological Chemistry* **193**, 265–275.
- Lwanga, E. H., Gertsen, H., Gooren, H., Peters, P., Salanki, T., van der Ploeg, M., Besseling, E., Koelmans, A. A. & Geissen, V. 2017 Incorporation of microplastics from litter into burrows of *Lumbricus terrestris*. *Environmental Pollution* **220**, 523–531.
- Mahdian, M., Hosseinzadeh, M., Siadatmousavi, S. M., Chalipa, Z., Delavar, M., Guo, M., Abolfathi, S. & Noori, R. 2023 Modelling impacts of climate change and anthropogenic activities on inflows and sediment loads of wetlands: Case study of the Anzali wetland. *Scientific Reports* **13**, 5399.
- Mintenig, S. M., Löder, M. G. J., Primpke, S. & Gerdt, G. 2019 Low numbers of microplastics detected in drinking water from ground water sources. *Science of the Total Environment* **648**, 631–635.
- Munno, K., Helm, P. A., Jackson, D. A., Rochman, C. & Alina Sims, A. 2018 Impacts of temperature and selected chemical digestion methods on microplastic particles. *Environmental Toxicology and Chemistry* **37** (1), 91–98.
- Muthuselvi, C., Pandiarajan, S. S., Ravikumar, B., Athimoolam, S., Srinivasan, S. & Krishnakumar, R. V. 2018 FT-IR and FT-Raman spectroscopic analyzes of Indeno Quinoxaline derivative crystal. *Asian Journal of Applied Sciences* **11** (2), 83–91.



- Nanthini devi, K., Santhanam, P. & Perumal, P. 2022 Impacts of microplastics on marine organisms: Present perspectives and the way forward. *The Egyptian Journal of Aquatic Research* **48** (3), 205–209.
- Novotna, K., Cermakova, L., Pivokonska, L., Cajthaml, T. & Pivokonsky, M. 2019 Microplastics in drinking water treatment – Current knowledge and research needs. *Science of the Total Environment* **667**, 730–740.
- Nwuzor, I. C., Oyeoka, H. C., Nwanonenyi, S. C. & Ihekwe, G. O. 2023 Biodegradation of low-density polyethylene film/plasticized cassava starch blends with central composite design for optimal environmental pollution control. *Journal of Hazardous Materials Advances* **9**, 100251.
- Oßmann, B. E., Sarau, G., Holtmannspötter, H., Pischetsrieder, M., Christiansen, S. H. & Dicke, W. 2018 Small-sized microplastics and pigmented particles in bottled mineral water. *Water Research* **141**, 307–331.
- Peng, B. Y., Sun, Y., Li, P., Yu, S., Xu, Y., Chen, J., Zhou, X., Wu, W. & Zhang, Y. 2023 Biodegradation of polyvinyl chloride, polystyrene, and polylactic acid microplastics in *Tenebrio Molitor* larvae: Physiological responses. *Journal of Environmental Management* **345**, 118818.
- Pivokonsky, M., Cermakova, L., Novotna, K., Peer, P., Cajthaml, T. & Janda, V. 2018 Occurrence of microplastics in raw and treated drinking water. *Science of the Total Environment* **643**, 1644–1651.
- Rizzarelli, P., Rapisarda, M., Perna, S., Mirabella, E. F., La Carta, S., Puglisi, C. & Valenti, G. 2016 Determination of polyethylene in biodegradable polymer blends and in compostable carrier bags by Py-GC/MS and TGA. *Journal of Analytical and Applied Pyrolysis* **117**, 72–81.
- Shahmoradi, A. R., Talebibahmanbigloo, N., Javidparvar, A. A., Bahlakeh, G. & Ramezanzadeh, B. 2020 Studying the adsorption/inhibition impact of the cellulose and lignin compounds extracted from agricultural waste on the mild steel corrosion in HCl solution. *Journal of Molecular Liquids* **304**, 112751.
- Shirazi, S., Mafighlami, R., Moghimi, H. & Borghei, S. M. 2023 Feasibility study of microplastic biodegradation in effluents from South Tehran WWTP after quantitative and qualitative measurement of the particles. *Applied Water Science* **13**, 80.
- Stride, B., Abolfathi, S., Odara, M. G. N., Bending, G. D. & Pearson, J. 2023a Modeling microplastic and solute transport in vegetated flows. *Water Resources Research* **59** (5), e2023WR034653.
- Stride, S., Dykes, C., Abolfathi, S., Jimoh, M., Bending, G. D. & Pearson, J. 2023b Microplastic transport dynamics in surcharging and overflowing manholes. *Science of the Total Environment* **899**, 165683.
- Tiwari, N., Santhiya, D. & Sharma, J. G. 2023 Degradation of polyethylene microplastics through microbial action by a soil isolate of *Brevibacillus brevis*. *Polymer Degradation and Stability* **2015**, 110436.
- Tiwari, N., Santhiya, D. & Sharma, J. G. 2024 Significance of landfill microbial communities in biodegradation of polyethylene and nylon 6,6 microplastics. *Journal of Hazardous Materials* **462**, 132786.
- Visentin, M., Stea, S., de Clerico, M., Reggiani, M., Fagnano, C., Squarzone, S. & Toni, A. 2006 Determination of crystallinity and crystal structure of Hylamer™ polyethylene after in vivo wear. *Journal of Biomaterials Applications* **21** (2), 131–145.
- Żwierello, W., Maruszewska, A., Skórka-Majewicz, M., Goschorska, M., Baranowska-Bosiacka, I., Dec, K., Styburski, D., Nowakowska, A. & Gutowska, I. 2020 The influence of polyphenols on metabolic disorders caused by compounds released from plastics–review. *Chemosphere* **240**, 124901.

First received 30 August 2023; accepted in revised form 23 October 2023. Available online 13 November 2023